Quaternary Science Reviews 27 (2008) 1442–1452

Contents lists available at ScienceDirect

Quaternary Science Reviews

journal homepage: www.elsevier.com/locate/quascirev

Millennial- and centennial-scale vegetation and climate changes during the late Pleistocene and Holocene from northern New Mexico (USA)

Gonzalo Jiménez-Moreno [a,b,c,*], Peter J. Fawcett [b], R. Scott Anderson [a]

[a] Center for Environmental Sciences and Education, Quaternary Sciences Program, Northern Arizona University, Flagstaff, AZ 86011, USA
[b] Department of Earth and Planetary Sciences, Northrop Hall, University of New Mexico, Albuquerque, NM 87131, USA
[c] Departamento de Estratigrafía y Paleontología, Universidad de Granada, Fuente Nueva s/n, 18002 Granada, Spain

ARTICLE INFO

Article history:
Received 21 January 2008
Received in revised form
8 April 2008
Accepted 9 April 2008

ABSTRACT

High-resolution pollen and magnetic susceptibility (MS) data from a sediment core from an alpine bog (3100 m) in the Sangre de Cristo Mountains (New Mexico) record variations in treeline elevation and in sedimentation for the last 14 ka (cal yr BP). Strong correspondence between the paleovegetation and the MS profile suggests that both records can be used to reconstruct past climatic conditions. The coldest conditions in this area occurred at the end of the late Pleistocene during the Pinedale glaciation and the Younger Dryas chron. A general warming trend took place during the early Holocene, lasting until ~5.6 ka, when the warmest conditions occurred. A progressive climate cooling is then observed until today. Millennial- and centennial-scale changes are also observed throughout the vegetation and MS records. The higher amplitude millennial-scale cold events appear to correlate with the timing and duration of episodes of enhanced sea-ice drift in the North Atlantic and the lower amplitude centennial-scale cold events may correlate with periods of lower solar activity. A solar-climate connection is suggested from these records by a prominent ca 200-yr cycle in tree pollen abundance, which may correlate with the 208 yr Suess solar cycle. This study shows an immediate response of the vegetation (treeline) to climate change at millennial- and centennial-scales, probably related to variations in summer insolation and solar activity during the late Pleistocene and Holocene. Such high-resolution studies are very important in order to predict future climate change and particularly in very arid areas, where human activity and economies are strongly influenced by climate.

© 2008 Elsevier Ltd. All rights reserved.

1. Introduction

A better understanding of past climate variability at shorter timescales is very important in order to understand natural climate variability upon which anthropogenic climate change is superimposed. This is especially true for the arid southwestern United States, whose population and economy is vulnerable to a variable precipitation regime. However, a scarcity of continuous, high-resolution postglacial climatic records currently exists for this area (Asmeron et al., 2007), the results of which could be drawn upon to assist in planning for the ecosystem changes that are occurring there. To provide the data necessary to understand past climate changes, many investigators have used high-resolution analyses of proxies from lakes and bogs, which can be very sensitive recorders of past climate changes (e.g., Anderson and Smith, 1994; Hodell et al., 2001; Hu et al., 2003; Jiménez-Moreno et al., 2007).

This paper is an interpretive report comparing pollen and magnetic susceptibility (MS) data from Stewart Bog, one of several alpine bogs and lakes within a suite of moraines at ~3100 m, 2 km below a cirque in the Winsor Creek Basin on the eastern flank of the Sangre de Cristo Mountains north of Santa Fe, NM, USA. The glacial history of this basin was first studied by Wesling (1988). Later, Armour et al. (2002) obtained and described the sedimentology, stratigraphy, and MS of six sediment cores from Stewart Bog. The cores record six glacial and periglacial events over the past 14,000 yr as discrete coarser clastic sedimentary layers with higher MS, which were correlated with millennial-scale climate change and ice rafting events in the North Atlantic (Armour et al., 2002). Here, we report on pollen analyses from one of the cores (B1-5). Today, upper treeline in the Sangre de Cristo Mountains occurs at an average elevation of ~3500 m, so the pollen stratigraphy from Stewart Bog should be sensitive to changes in the composition of subalpine communities and the elevation of upper treeline, which are primarily sensitive to the length and relative warmth of the growing season. We interpret this pollen

* Corresponding author at: Center for Environmental Sciences and Education, Quaternary Sciences Program, Northern Arizona University, Flagstaff, AZ 86011, USA. Tel.: +1 505 280 8764; fax: +1 505 277 8843.
E-mail address: gonzaloj@ugr.es (G. Jiménez-Moreno).

0277-3791/$ - see front matter © 2008 Elsevier Ltd. All rights reserved.
doi:10.1016/j.quascirev.2008.04.004

stratigraphy to re-evaluate the links between vegetation, climate and hydrology of Stewart Bog at both millennial- and centennial-scales.

1.1. Geomorphic setting

The Winsor Creek drainage basin is located ~60 km northeast of Santa Fe, NM, on the eastern flank of the Santa Fe Range (Fig. 1). The uppermost part of the basin contains four cirques, the principal one containing Lake Katherine. These cirques are oriented east to northeast with steep slopes on their southern and southwestern sides. Wesling (1988) established the glacial chronology for this basin using moraine relative age data, including soil-profile development and degree of clast weathering and landform preservation. He assigned a Pinedale age to a moraine suite at 3100 m in the middle drainage containing small lakes and bogs, including Stewart Lake and Stewart Bog and a late Pinedale age to moraines farther upvalley. A moraine currently damming Lake Katherine at 3580 m was assigned a late Pleistocene to early Holocene age based on a more juvenile soil profile and steeper slopes than the classic Pinedale deposits. An inset lateral moraine-like feature within the Lake Katherine cirque with little soil development and a very sharp surface profile was assigned a late Holocene age based on a radiocarbon date of 3570 ± 145 ^{14}C yr BP from charcoal underlying this feature (Wesling, 1988).

1.2. Vegetation

The forest composition of the Sangre de Cristo Mountains in New Mexico is similar to other forests of the southern Rockies (Peet, 1988), with species composition and forest structure dependent upon a complex mix of elevational gradients, topographic position and disturbance history (Allen and Peet, 1990). *Pinus edulis* (Colorado piñon)—*Juniperus monosperma* (oneseed juniper) woodlands occur on the lower slopes of the range. An upper montane coniferous forest, from 2400 to 3100 m, features *Pseudotsuga menziesii* (Douglas-fir), *Abies concolor* (white fir), *Pinus strobiformis* (southwestern white pine), *P. ponderosa* (ponderosa pine), *Picea pungens* (Colorado blue spruce), *Quercus gambelii* (Gambel oak) and *Acer glabrum* (Rocky Mountain maple). Above ~3100 m, a subalpine coniferous forest occurs with *Picea engelmannii* (Engelmann spruce), *Abies lasiocarpa* (subalpine fir) and *Pinus aristata* (bristlecone pine) as the most diagnostic trees, but also *P. menziesii*, *P. strobiformis*, *Populus tremuloides* (aspen) and *Juniperus communis* (common juniper). Treeline elevation in the Sangre de Cristo Mountains is ~3500 m and vegetation above is characterized by alpine tundra, dominated by compact low-growing perennials such as *Artemisia scopulorum* (alpine sage), *Geum rossii* (alpine avens), *Polygonum bistortoides* (bistort), *Tonestus pigmaeus* (cushion yellow aster), *Festuca brachyphylla* (alpine fescue), *Arenaria fendleri* (sandwort), *Carex rupestris* (sedge), *Salix arctica* (willow) and *S. reticulata* (willow). [Terminology primarily follows Dick-Peddie (1993), and Weber and Wittman (1996)]. Stewart Bog is located at 3100 m, at the transition to the subalpine coniferous forest.

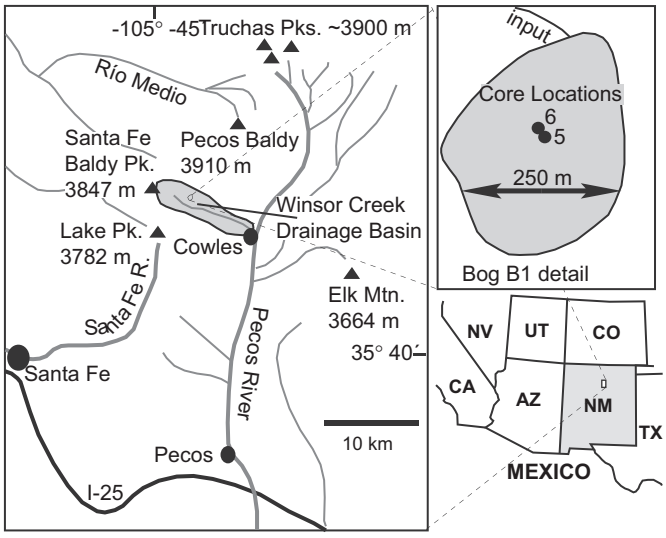

Fig. 1. Sketch map of Winsor Creek drainage basin, Sangre de Cristo Mountains, New Mexico. Insets show study area location and Stewart Bog detail with core B1-5 and B1-6 locations.

2. Materials and methods

2.1. Sediment collection and stratigraphic correlations

Six sediment cores were obtained from Stewart Bog using a Livingstone square-rod piston corer (Armour et al., 2002). The entire sequence of late Pleistocene to Holocene sediment was recovered in three (B1-4, B1-5, and B1-6) of the six cores, and sedimentologic and stratigraphic features were observed and noted for each (Armour et al., 2002; core B1-5 is shown in Fig. 2). These cores record the evolution of a small alpine lake to a bog, punctuated by discrete sedimentary events that were interpreted as reflecting colder climate episodes (Armour et al., 2002).

In the Armour et al. (2002) study, greater emphasis was placed on analysis of core B1-6. Little sediment remained after those analyses, so our analyses come from core B1-5. Although we obtained several ^{14}C ages for core B1-5 (see Table 1), we used several dates obtained from core B1-6 for the B1-5 chronology since the two cores were taken only 1 m apart, and the stratigraphies and MS profiles are nearly identical. Armour et al. (2002) provided detailed stratigraphic descriptions

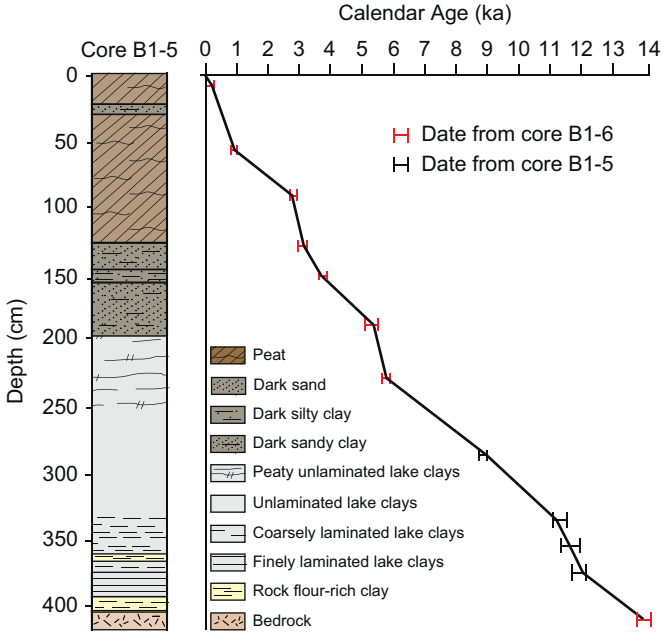

Fig. 2. Lithology of the B1-5 core and age-depth diagram with 2σ ranges in error bars. Dates come from core B1-5 and an adjacent core (B1-6) with a nearly identical stratigraphy (see legend and Table 1 for more explanation and Armour et al., 2002 for stratigraphic correlations).

Table 1
Radiocarbon dates from cores B1-5 and B1-6

Lab no.[a]	Core	Depth (cm) B1-5[b]	Material dated	Radiocarbon date (^{14}C yr BP $\pm 1\sigma$)	Calibrated age (cal BP) 2σ ranges
AA-35802	B1-6	8	Bulk peat	120±60	0–274
AA-35801	B1-6	56	Bulk peat	990±35	795–963
AA-35800	B1-6	90	Charcoal	2770±45	2767–2964
AA-35799	B1-6	127	Bulk peat	2950±45	2965–3256
AA-35795	B1-6	149	Wood	3495±50	3640–3889
AA-35794	B1-6	186	Charcoal	4550±50	5041–5444
AA-35798	B1-6	225	Grassy sediment	5010±50	5644–5900
UCIAMS-32510	B1-5	282	Wood	7955±20	8726–8981
Beta-153457	B1-5	330	Bulk sediment	9890±60	11,200–11,602
Beta-153454	B1-5	347	Charred wood	10,070±60	11,334–11,963
Beta-153455	B1-5	370	Charred wood	10,180±50	11,629–12,063
AA-35802	B1-6	404	Bulk sediment	12,120±95	13,768–14,189

All ages were calibrated using CALIB 5.0 (Stuiver and Reimer, 1993).
[a] Sample number assigned at radiocarbon laboratory; AA# = NSF-Arizona AMS facility, Beta# = Beta Analytic, Inc., UCIAMS# = University of California at Irvine W.M. Keck Carbon Cycle Accelerator Mass Spectrometry Laboratory.
[b] Positions of radiocarbon dates in core B1-5 from core B1-6 were inferred by direct correlation using MS data (Armour et al., 2002).

and explanations for the core correlations, so we concentrate only on core B1-5 here.

A decimeter-thick unit of light-grey-yellowish, glacial flour-rich massive clay rests on top of the basal granitic bedrock (talus) (Fig. 2). This unit is overlain by greyish lake clays that grade upwards from finely laminated to coarsely laminated to massive which finally become very peaty at the top. This unit is interrupted at 361 cm by a second ca 5-cm light flour-rich massive clay. The lake clays are overlain at 200 cm by dark sandy and silty clays very rich in vegetal remains and at 130 cm the sediments became mostly organic with the deposition of dark-brown peat. A 3-cm thick sandy silt level is recorded at 26.8 cm depth (Fig. 2).

2.2. Pollen and magnetic susceptibility

The 4.1 m-long core B1-5 was sampled continuously at 2 cm intervals (~60 yr) for pollen analysis, from the same samples taken for MS analyses (Armour et al., 2002). Pollen extraction methods followed a modified Faegri and Iversen (1989) technique, including treatment with KOH, washing through a 180-μm screen, and treatment with dilute HCl, HF and acetolysis solution. Grains were stained with Safranin O, and mounted in silicone oil. Counting was performed at 400× magnification on a compound light microscope. Pollen identification was accomplished to the lowest taxonomic level possible by comparing the fossils with their present-day relatives using published keys and the modern pollen reference collection at Northern Arizona University. *P. edulis* (piñon) pollen was differentiated from the rest of *Pinus* pollen by its smaller size (generally lesser than 65 μm in breadth) and the presence of verrucae on the leptoma. The pollen sum included all upland pollen taxa, and excluded the aquatics [*Alnus* (alder), *Salix*, Cyperaceae (sedge), Apiaceae (parsley family), Liliaceae (lily family) and Ranunculaceae (buttercup family)]. The results were plotted using Adobe Illustrator, and zoned using CONISS (Grimm, 1987) using the following pollen types: *Pinus*, *Picea*, *Abies*, *Artemisia*, Poaceae, Cheno-ams and aquatics as a group (*Alnus*, *Salix*, Cyperaceae, Apiaceae, Liliaceae and Ranunculaceae) (Fig. 3).

To highlight basic patterns in subalpine tree taxa, *Abies*, *Picea* and *Pinus* were grouped together and plotted in Fig. 4C. We also calculated the ratio of *Picea* to *Artemisia* (P/A ratio) (Fig. 4B). Other investigators (Maher, 1972; Toney and Anderson, 2006) have used this ratio to investigate potential changes in pollen sedimentation. We use this ratio here to track changes in treeline, since *Artemisia* is an important alpine species locally. We added a seven-point average curve to the raw pollen and MS data to make the changes more clear, avoiding misinterpretations given by small variability (Fig. 4). Since modern pollen studies over an elevational gradient are rare for the southern Rockies (Shafer, 1989; Hall, 1990; Fall, 1992), complicating paleoenvironmental interpretations of the Stewart Bog record, we also base our interpretations of the pollen record from Stewart Bog on several studies from sediment cores from nearby areas that show a direct relationship between percentage of subalpine trees in the pollen spectra and paleoelevation of treeline with respect to the study site (Carrara et al., 1984; Reasoner and Jodry, 2000; Toney and Anderson, 2006).

Magnetic susceptibility was measured at the University of New Mexico paleomagnetism laboratory using a Sapphire Instruments SI-2 induction coil by Armour et al. (2002). Previously, core B1-5 was sampled using 8 cm^3 plastic cubes with embossed arrows. Oriented samples were pre-cut with Cu–Be (non-magnetic) tools and then placed in the cubes, which were stored in a magnetic shielded container and refrigerated. MS was measured twice, with air correction measurements made four times in order to normalize each sample against background, and then each pair of sample measurements was averaged.

2.3. Spectral analysis

A cyclostratigraphic analysis was performed on the B1-5 pollen time series. We used the program REDFIT (Schultz and Mudelsee, 2002) with the objective of characterizing the different periodicities present in the unevenly spaced pollen time series and estimating its red-noise spectra. The spectral analysis assisted in identifying recurrent features or periodicities through spectral peaks registered at differing frequencies throughout the studied core. Cross-spectral analysis (using SPECTRUM; Schulz and Stattegger, 1997) of (1) the P/A ratio and MS from core B1-5 and (2) the residual Δ^{14}C data (Reimer et al., 2004) and detrended subalpine tree pollen abundance from core B1-5 was also performed in order to test for a relationship between (1) variations in vegetation and sedimentation in Stewart Bog and (2) variations in vegetation and climate in New Mexico and solar variability during the Holocene.

3. Results and discussion

3.1. Chronology

The chronology for core B1-5 core is based on 12 AMS radiocarbon dates, calibrated to calendar years (CALIB 5.0;

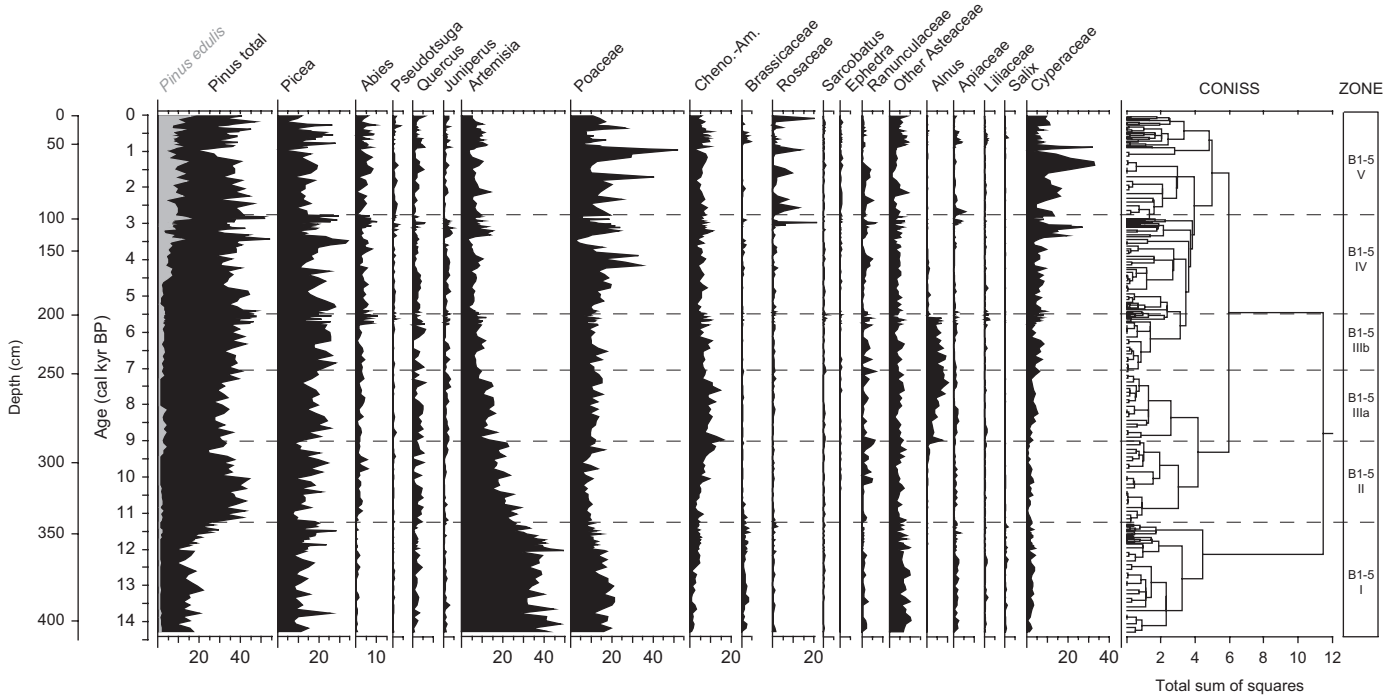

Fig. 3. Pollen diagram of the B1-5 core showing percentages of selected taxa. A minimum of 300 grains of terrestrial pollen was counted in every sample. The zonation was made using cluster analysis provided by CONISS (Grimm, 1987).

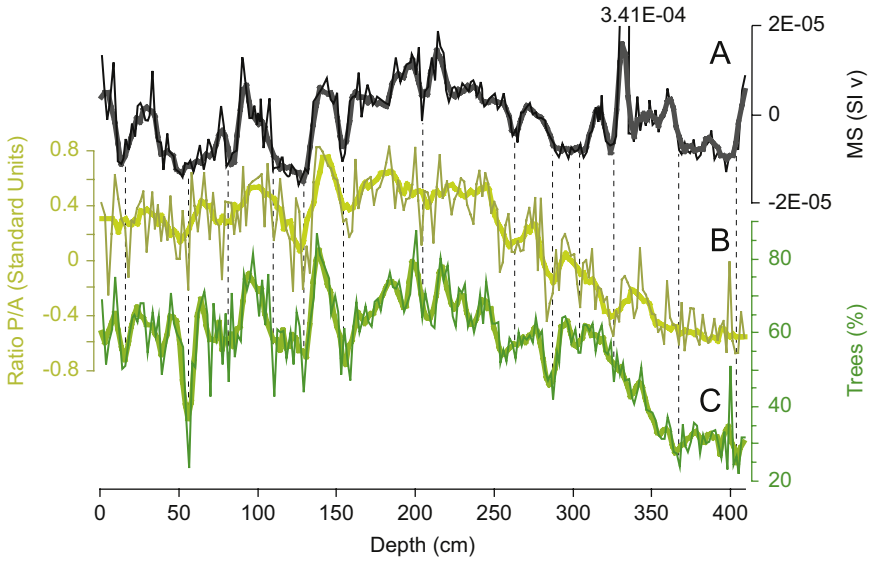

Fig. 4. Comparison of climate proxy records from core B1-5, Sangre de Cristo Mountains, New Mexico. (A) Magnetic susceptibility (MS) profile of sediment core B1-5 (Armour et al., 2002). (B) *Picea*/*Artemisia* (P/A) ratios in the pollen spectra from core B1-5. The P/A ratio is calculated as (P−A)/(P+A), where "P" represents percent *Picea* and "A" percent *Artemisia*. (C) Relative abundance of subalpine tree taxa (*Abies*, *Picea* and *Pinus*) in the pollen spectra. Low MS values generally correspond to low relative abundance of subalpine tree taxa and P/A ratios (dashed lines). Thin lines represent raw data and thick lines are the seven-point moving average.

http://calib.qub.ac.uk; Fig. 2). These include four dates directly from core B1-5 and eight dates from companion core B1-6 taken 1 m immediately north of B1-5. The 12 dates (Table 1) from cores B1-5 and B1-6 provide an age-depth curve that shows increasing age with depth (Fig. 2). No age reversals occur in the record, and so we chose the simplest linear age model, which includes all AMS dates (Fig. 2). The highest rate of sediment accumulation occurs between ca 90–127 cm (3100 and 2860 cal yr BP; 6.8 yr cm^{-1}), followed by ca 186–225 cm (5750–5175 cal yr BP; 14.8 yr cm^{-1}) and ca 330–370 cm (11,880–11,300 cal yr BP; 14.4 yr cm^{-1}). The latter of the three periods occurs near the end of the Younger Dryas period, and may be related to increased sediment flux during that period (Armour et al., 2002).

3.2. Pollen stratigraphy

Based upon the zonation of the pollen data (Fig. 3) we determined five pollen zones. These data provide a general framework for discussion of vegetation change in the Sangre de Cristo Mountains of New Mexico.

Zone B1-5-I (core bottom—340 cm; ca 14,500–11,200 cal yr BP). This zone encompasses the Lateglacial at Stewart Bog. Non-arboreal pollen types are most abundant at this time, including *Artemisia* (generally 30–40%), Poaceae (10–20%), Other Asteraceae (5–10%), and Brassicaceae (to ca 4%). *Picea* percentages generally vary between 10% and 15%; *Pinus* fluctuates between 10% and 20%, increasing substantially toward the end of the zone. Other arboreal pollen types—*Abies*, *Pseudotsuga* and *Juniperus*—occur in trace amounts, including *Quercus*, which makes up only 1–5% of the pollen sum.

These high non-arboreal, low *Picea* and *Pinus*, and trace *Abies* and *Pseudotsuga* pollen percentages suggest alpine tundra or steppe vegetation (Fall, 1992). However, pollen percentages of tree taxa suggest that *Picea* trees may have been present locally or near the bog, but *Pinus* trees probably were not. Unlike other proxies in the sedimentary record (Armour et al., 2002) vegetation change during the Younger Dryas is recorded only subtly, with maximum percentage of *Artemisia* in the pollen record between ca 12,200 and 11,500 cal yr BP (Fig. 3).

Zone B1-5-II (ca 340–285 cm; 11,200–9000 cal yr BP). During the early Holocene, *Pinus* percentages increase substantially (to over 40%), while most non-arboreal types—including *Artemisia* and Poaceae—decline. The decline in *Artemisia* is quite gradual however (Fig. 3), suggesting its continued importance on the landscape. Subalpine conifers—particularly *Abies* (to 5%)—increase, as does pollen from *Quercus* (to 5%) and Cheno-Ams (5–10%).

Comparison with modern pollen studies (Shafer, 1989; Hall, 1990; Fall, 1992) shows substantial matches with modern subalpine forest, dominated by *Picea* and *Abies*. It also suggests a major expansion of *Pinus* and *Quercus* forest or woodland somewhere near the site (Shafer, 1989), but probably at lower elevations. Percentages of Chenopodiaceae pollen (perhaps *Atriplex*) are characteristic of much lower elevations, within the *P. edulis*/*Juniperus* woodland (Shafer, 1989) or within the High Plains grassland to the east (Hall, 1990). It is unlikely, for instance, that *Quercus* or *Atriplex* grew near the Stewart Bog site. Comparable percentages of these pollen types are deposited today within the subalpine environment, even though no individual plants occur locally (Hall, 1990; Fall, 1992). The increase in *Pinus* may be from an expansion of *P. ponderosa* forests within the modern montane zone (Hall, 1990), noted also in other records from the southern Rockies at this time (Reasoner and Jodry, 2000; Toney and Anderson, 2006; Anderson et al., 2008a, b).

Zone B1-5-III (ca 285–200 cm; 9000–5500 cal yr BP). Pollen spectra dating to the early-to-middle Holocene clusters in two subzones—B1-5-IIIa (ca 9000–7100 cal yr BP) and B1-5-IIIb (ca 7100–5500 cal yr BP). In the older subzone, *Picea*, *Abies*, *Pinus* and *Quercus* pollen remains high, and *Artemisia* continues to decline. However, Poaceae and Cheno-Am (cf. *Atriplex*) pollen begin to increase (the latter to reach maximum Holocene values of 10–15%), with minor increases in pollen of *P. edulis*-type (piñon) and *Juniperus*. *Alnus* expands dramatically in the pollen record (Fig. 3), and remains up to 10% of the sum for the entire zone before declining. Cyperaceae pollen begins a steady increase that culminates in the late Holocene. In subzone B1-5-IIIb, both *Picea* and *Pinus* increase from ca 20% to 28% and ca 35% to 42%, respectively.

Like B1-5-II, pollen spectra from B1-5-III are most similar to modern pollen spectra from the subalpine zone. However, we interpret the increase in pollen types characteristic of more arid, lower elevation scrublands (e.g., Cheno-Ams, probably *Atriplex*) along with Poaceae, to indicate expansion of those communities at elevations below Stewart Bog, especially from ca 9000 to 7100 cal yr BP, probably to the west and east of the Sangre de Cristo range (Hall, 1990). The large increase in *Alnus*, and the gradual increase in Cyperaceae, pollen suggests that the small lake transitioned to a marsh during this time, and then to a bog after ca 5500 cal yr BP. This is also clearly seen in the stratigraphy of the core (Fig. 2). Thus, the period of ca 7100–5500 cal yr BP may have been the driest period of the Holocene. Evidence from other sites throughout the southwest substantiates this conclusion.

Zone B1-5-IV (ca 200–95 cm; 5500–2800 cal yr BP). This transition from the mid- to the late Holocene witnessed a change in deposition of both arboreal and non-arboreal pollen. Percentages of *Picea* and *Pinus* are both generally less than before, while Poaceae generally increases. *Abies* pollen nearly doubles to 6% after ca 6000 cal yr BP, and *Pseudotsuga* and *P. edulis* percentages also increase. *Artemisia* pollen reaches a minimum for the record during this zone, and although Cyperaceae pollen continues to increase, *Alnus* pollen essentially disappears from the record.

Again, the best matches of the fossil pollen spectra with modern data are from the subalpine forests (Shafer, 1989; Hall, 1990; Fall, 1992). But the relatively large fluctuations in *Picea*, *Pinus* and Poaceae pollen (Fig. 3) suggest either a change in deposition process, or perhaps an increase in site disturbance. We do not know from the pollen data whether the increased pollen of Poaceae comes from wetland or terrestrial sources, but at least the increase in Cyperaceae is consistent with increased paludification of the site coincident with neoglacial activity (Wesling, 1988; Armour et al., 2002) within the southern Rockies and Sangre de Cristo range at this time.

Zone B1-5-V (ca 95 cm—surface; 2800 cal yr BP—present). During the latest Holocene, *Picea*, *Pinus* and *Abies* continue to dominate the pollen record (Fig. 3). *Pseudotsuga* pollen percentages attain their Holocene maxima (at ca 2%). *P. edulis* pollen also reaches a sustained Holocene maximum (10–15%), begun during Zone B1-5-IV, while *Artemisia* pollen percentages are variable from ca 7% to 10%. Other non-arboreal pollen types are abundant, including Poaceae, Rosaceae, Apiaceae and Cyperaceae.

Comparison to available modern pollen samples suggests that the surrounding forest may have "thinned" in the sense that higher percentages of non-arboreal pollen types and pollen of trees from lower elevations (e.g., *Pseudotsuga*, *P. edulis*) were deposited, suggesting a more open subalpine vegetation during this time. However, the increase in *P. edulis* pollen is widespread regionally (Anderson et al., 2008a, b), and has been attributed to climatic factors (Holmgren et al., 2007). The occurrence specifically of Apiaceae and Cyperaceae suggest continued paludification of the sites throughout the late Holocene. But the alternation of high pollen percentages from Poaceae and Cyperaceae suggests to us that the bog alternated between wetter (Cyperaceae) and drier (Poaceae) states.

3.3. Paleoclimate implications

Because alpine treeline is primarily sensitive to temperature and length of the growing season (Cairns and Malanson, 1998), movements upslope or downslope of high elevation tree species, as recorded in percentage variations of arboreal pollen in alpine lake records, can be good proxies for temperature change. Several studies from the southern Rocky Mountains (Markgraf and Scott, 1981; Carrara et al., 1984, 1991; Reasoner and Jodry, 2000; Toney and Anderson, 2006) have used this relationship to document treeline fluctuations during the Holocene.

Our detailed analysis demonstrates that large fluctuations occur in the pollen spectra, as well as the MS in the Stewart Bog B1-5 record (Figs. 4 and 5). Large-amplitude variations in magnetic properties documenting changes in the sedimentary input were previously interpreted by Armour et al. (2002) as climatically driven fluctuations in precipitation and/or glacial

runoff. In order to simplify the comparisons, we combined the subalpine tree (arboreal) taxa (*Picea*, *Pinus* and *Abies*) and calculated the P/A ratio to compare with the MS data. A correlation coefficient (r) between the P/A ratio and the MS was also calculated in order to quantify this relationship (Fig. 6). The MS variations are mostly synchronous with changes in these taxa, which represent changes in subalpine vegetation and *Artemisia* tundra or steppe vegetation (Fig. 4). Increases in arboreal (tree) pollen and in the P/A ratio (Figs. 4 and 5F and G), likely indicating a warming-induced upslope displacement of alpine treeline (as discussed above) are generally associated with increases in MS (Figs. 4 and 5H), denoting periods of enhanced clastic deposition in the basin. A positive correlation coefficient of $r = 0.47$ between 0 and 5 ka and $r = 0.69$ between 5 and 10 ka confirms this relationship for most of the Holocene (Fig. 6A and B). Often, high concentrations of charcoal (not shown here) accompany these fluctuations, and suggest that enhanced fire-induced erosion (e.g., Pierce et al., 2004; Pierce and Meyer, 2008) during warm periods could have contributed to this positive correlation. Conversely, decreases in tree pollen and increases in pollen probably originating from alpine tundra or steppe environments (mainly *Artemisia*, Poaceae and Rosaceae) (Figs. 3–5F and G) likely indicate a downslope displacement of the alpine treeline. These periods are associated with decreases in the MS values (Figs. 4 and 5G) and a lack of charcoal. We interpret this as denoting periods of lower clastic sedimentation in the basin and suppression of fire-induced erosion in the basin during cold periods.

In this study, we show that the lower amplitude MS variations during the Holocene are most likely related to changes in sedimentary input into the basin associated with variations in fire-induced erosion. The link between fire and increased warmth and/or drought has been clearly demonstrated (Pierce et al., 2004; Frechette, 2007; Pierce and Meyer, 2008). In contrast, the larger amplitude MS variations in the late Holocene discussed in Armour et al. (2002), correlate with distinct changes in sedimentary facies, usually coarser sedimentary units such as sands and gravels.

The lowest subalpine pollen percentage and P/A ratio—and, in our interpretation, the coldest event—is recorded at ca 14 ka

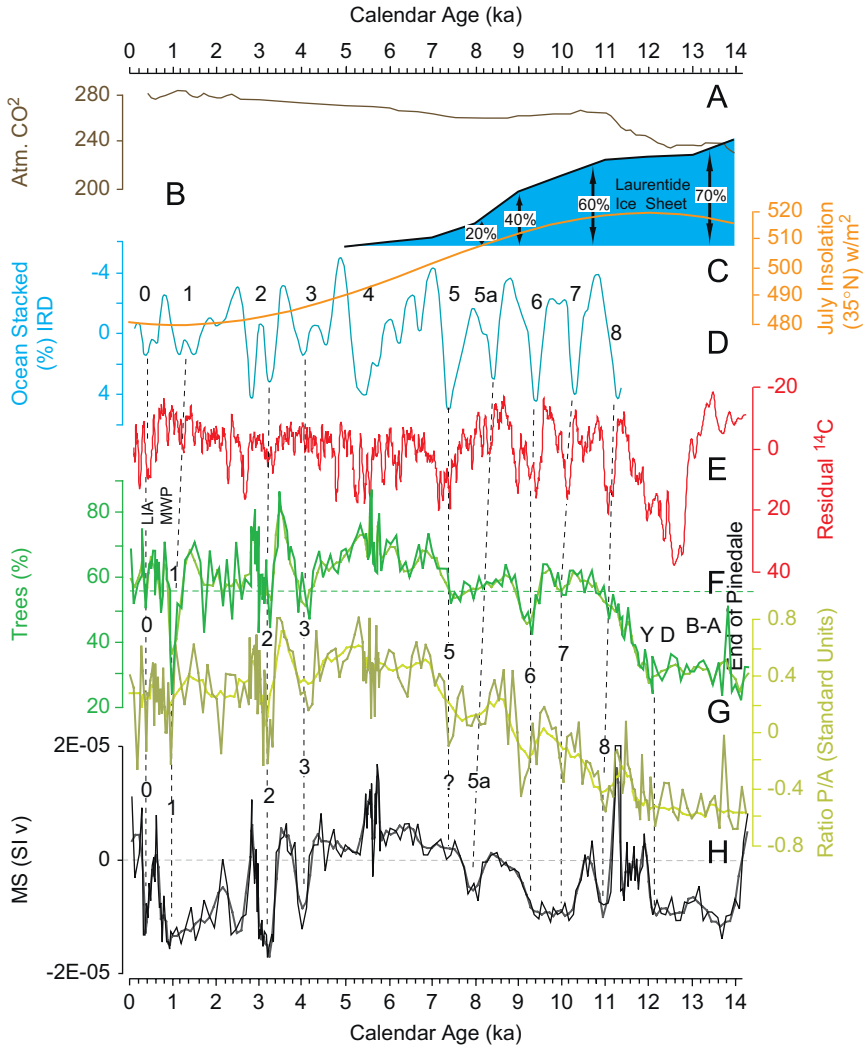

Fig. 5. Comparison of proxy records of climate change and solar activity for the last 14 ka. (A) Atmospheric carbon dioxide concentration from Shuman et al. (2005). (B) Area of the Laurentide ice sheet as a fraction of the area during the Last glacial maximum (LGM) from Shuman et al. (2005). (C) July insolation at 35°N (Laskar, 1990). (D) Stacked marine ice rafting debris (IRD) records in percentage from the North Atlantic (Bond et al., 2001). Cold events are marked with numbers from 0 to 8 (Bond et al., 2001). (E) Residual $\Delta^{14}C$ data calculated from IntCal04 $\Delta^{14}C$ (‰) with a 2000-yr moving average subtracted (Reimer et al., 2004). (F) Relative abundance of subalpine tree taxa (*Abies*, *Picea* and *Pinus*) in the pollen spectra from core B1-5. Numbers point to main cooling events. LIA, MWP, YD, B-A are Little Ice Age, Medieval Warm Period, Younger Dryas and Bølling-Allerød, respectively. (G) *Picea*/*Artemisia* (P/A) ratios in the pollen spectra from core B1-5. The P/A ratio is calculated as (P–A)/(P+A), where "P" represents percent *Picea* and "A" percent *Artemisia*. (H) Magnetic susceptibility (MS) profile of sediment core B1-5 (Armour et al., 2002). Thin lines represent raw data and thick lines are the seven-point moving average.

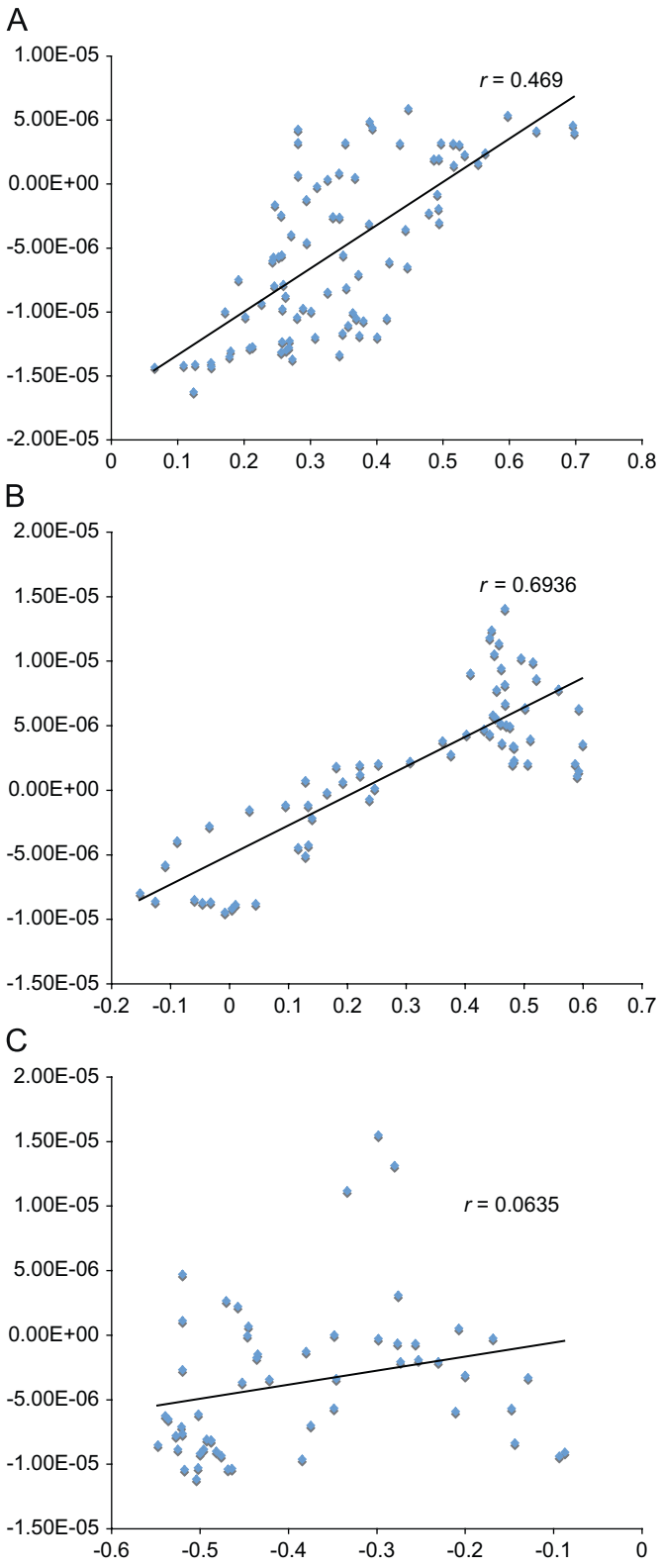

Fig. 6. Correlation plots of the seven-point average P/A ratio and MS from core B1-5 from (A) 0–5 ka, (B) 5–10 ka and (C) 10–14 ka. Correlation coefficient (r) is given in each plot.

(1 ka = 1000 cal yr BP), corresponding to the local expression of the terminal Pinedale glaciation and lowered treeline (Fig. 5F and G). Increases (ca 10%) in subalpine tree taxa between 13.8 and 12.8 ka occurred during the Bølling-Allerød warm interval, supporting our interpretation of a climatic explanation. A subsequent decline in the subalpine tree taxa and the P/A ratio, with a minimum at ca 12 ka, coincides with the Younger Dryas cold interval. A low positive P/A ratio–MS correlation coefficient of $r = 0.0635$ between 10 and 14 ka (Fig. 6C) indicates a poor correlation between the changes in the vegetation and the changes in the MS for the late Pleistocene and the earliest Holocene, showing a different mechanism controlling the sedimentation in the basin than the one explained above and probably more related to glacial sedimentary dynamics. However, MS data show a similar pattern to the pollen which was also interpreted by Armour et al. (2002) as the Lateglacial–Holocene transition with a Younger Dryas cooling followed by an abrupt termination (Fig. 5H). The large MS spike at around 11.3 ka was interpreted by Armour et al. (2002) as the product of a breach in the Lake Katherine moraine that produced a large flood that washed glacial debris into the basin at the end of the glacial advance. The timing and direction of these changes during the Bølling-Allerød-to-Younger Dryas transition are nearly identical to those elsewhere in the southern Rockies (Reasoner and Jodry, 2000).

The early Holocene climate was characterized by increasing tree pollen percentages, upslope migration of the alpine treeline, and a warming of climate (Fig. 5F and G), probably in response to an increase in summer insolation (Kutzbach et al., 1998; Fig. 5C) and its influence on summer temperatures. The pollen changes during this time period are very similar to those from other locations in the southern Rockies (e.g., Little Molas Lake, Toney and Anderson, 2006; Black Mountain Lake and Sky Pond, Reasoner and Jodry, 2000), suggesting regional development of the subalpine forests at this time. Further, several studies (Carrara et al., 1984, 1991; Feiler et al., 1997; Anderson et al., 1999) suggest conditions warm enough at this time to allow treeline to expand to higher elevations. This overall warming trend in the early Holocene was punctuated by several brief cold events, discussed below.

The pollen data suggest that warm conditions continued until ca 5.6 ka, when the highest percentage of subalpine tree pollen, and consistently high MS and P/A values were recorded. This may have been the warmest part of the Holocene in the Sangre de Cristo Mountains as elsewhere in the southern Rockies. In the nearby San Juan Mountains of southern Colorado, treeline remained higher (Carrara et al., 1984) and some lakes showed lower Holocene lake levels (Toney and Anderson, 2006; Anderson et al., 2008a) at this time compared to present. In the Jemez Mountains of northern New Mexico, groundwater tables lowered, leading to a disconformity in peat accumulation (Anderson et al., 2008b). In northern Arizona, the mid-Holocene also documents lowest lake levels on the North Rim (Weng and Jackson, 1999), and the period of highest temperatures at Montezuma Well, Arizona (Davis and Shafer, 1992). Further south in New Mexico, the mid-Holocene witnessed abundant fire-related alluvial fan deposits in the Sacramento Mountains (Frechette, 2007) and extreme drought recorded by eolian landforms in Lake Estancia (Menking and Anderson, 2003), as well as maximum transport of Caribbean surface waters and moisture into the Gulf of Mexico associated with a stronger SW North American monsoon (Poore et al., 2003, 2005).

The highest July temperatures derived from $\delta^{13}C$ analysis in buried soils from North American Great Plains (Nordt et al., 2007) also occur at this time. The delay in thermal maximum from the early Holocene insolation maximum (Fig. 5C) may be related to the lingering effects of the Laurentide Ice Sheet (Kaufman et al., 2004) (Fig. 5B), a CO_2 concentration already at pre-industrial levels (Fig. 5A), and continued relatively high summer insolation (Fig. 5C) (Kutzbach et al., 1998). The marine record from the Gulf of Mexico (Poore et al., 2003, 2005) suggests that enhanced monsoonal circulation, and thus summer rainfall, may have

continued long into the middle Holocene in the Sangre de Cristo Mountains. This could enhance runoff in the basin and could explain the highest MS values in our record during the Holocene and the generally positive correlation between pollen and MS.

A progressive cooling trend indicated by a long-term decline in the percentage of subalpine tree pollen, P/A ratios and MS, began after the middle Holocene until present (Fig. 5F–H). This may result from a decrease in summer insolation (Kutzbach et al., 1998). *P. edulis* (piñon pine) and *Abies* increased considerably over this interval (Fig. 3), also regionally (Anderson et al., 2008a, b), indicating an increase in winter precipitation linked to enhanced and more frequent El Niño events during the last 5 ka (Friedman et al., 1988; Moy et al., 2002; Friddell et al., 2003; Rein et al., 2005) or to a combination of cooler summers and warmer winters from middle to late Holocene (Holmgren et al., 2007). In addition, the long-term increase in *Artemisia* in the B1-5 record is mirrored at other sites in the southern Rockies (Anderson et al., 2008a), particularly noted at the Alkali Basin, site in central Colorado (Markgraf and Scott, 1981). We interpret this as an expansion of *Artemisia* steppe in intermontane valleys, also reflecting cooler conditions.

Wesling (1988) described the presence of a late Holocene lateral moraine within the Lake Katherine cirque and interpreted it as a glacial advance. We suggest here that this feature could also be a protalus rampart that formed during a colder period during the late Holocene. The paleovegetation data shown here (Figs. 3 and 4) suggest a cooler climate period during the late Holocene, but not as cold as the late Pleistocene. The fact that this geomorphic feature is at the same elevation as the late Pleistocene (Younger Dryas) moraine would require similar glacial equilibrium line elevations (ELA) and this is not supported by the vegetation reconstructions.

3.4. Millennial- and submillennial-scale variability

In general, the co-located pollen and MS samples show good correlations between the Holocene climate events recorded in the Sangre de Cristo Mountains (core B1-5) as vegetation changes (subalpine tree pollen and P/A ratios) and MS. In the earlier Armour et al. (2002) study, millennial-scale cold events, interpreted from changes in sedimentology and MS, were correlated with cold events in the North Atlantic and Greenland for the middle to late Holocene. Here, we interpret multiple millennial- and centennial-scale cold events in the Sangre de Cristo Mountains based on the high-resolution vegetation reconstructions, particularly changes in subalpine tree pollen percentages and P/A ratios (Fig. 5). There appears to be a strong linkage between millennial-scale climatic variability and changes in North American vegetation communities during the Holocene (e.g., Davis and Shafer, 1992; Viau et al., 2002; Willard et al., 2005). For many plant communities, a rapid response (~50 yr lags) to multi-decadal- to centennial-scale climatic change is common (Shuman et al., 2005; Gray et al., 2006). The dense radiocarbon date chronology of cores B1-5 and B1-6 allow us to correlate many of these Holocene climatic changes in the Sangre de Cristo Mountains with climatic changes in the North Atlantic basin during the early Holocene as well as later in the Holocene.

Many of the Holocene climate variations recorded at Stewart Bog correlate within a century with large shifts in the ^{14}C production ($\Delta^{14}C$) rates (Fig. 5E) as well as with variations in sea-ice drifting in the North Atlantic (Bond et al., 2001) (Fig. 5D). Our interpreted warmer intervals in the Sangre de Cristo Mountains appear to generally correspond to intervals of high solar activity and to relatively warmer conditions in the subpolar North Atlantic (Bond et al., 2001). Conversely, interpreted colder intervals shown by lower subalpine tree pollen percentages, lower P/A ratios and reduced MS values generally correlate well with cooler periods in the North Atlantic within the radiocarbon date error (Fig. 5D), although not all cold events in New Mexico correlate with cold events in the North Atlantic and vice versa.

The most prominent early Holocene cold event recorded by subalpine tree pollen percent is centred at 9.3 ka, which occurs at the same time as cold event 6 in the North Atlantic (Fig. 5D; Bond et al., 2001), as well as during a lake highstand recorded in pluvial Lake Palomas, directly south in Chihuahua, Mexico (Castiglia and Fawcett, 2006). This event is also seen as a prominent decline in P/A ratios (Fig. 5F), but is not well expressed in the MS profile. Three additional early Holocene cold events are well resolved in the P/A profile and could be related to the 8.2 ka event, the 9.95 ka anomaly, and the Preboreal oscillation (Fig. 5E; Bond et al., 2001). The 8.2 ka event and the Preboreal oscillation are seen in the MS profile, but are not well expressed in the arboreal pollen profile.

Each of these early Holocene cold events have recently been recognized in a suite of ice cores from central Greenland (Johnson et al., 2001; Rasmussen et al., 2007) and within the dating errors of this record, appear to correlate with the cold events in the Sangre de Cristo Mountains reported here (Fig. 5). The 8.2 ka event has been widely recognized throughout the northern hemisphere (Alley et al., 1997) and is present in this record also. In Greenland, the 9.3 ka event is similar in amplitude although shorter in duration than the 8.2 ka event (Johnson et al., 2001; Rasmussen et al., 2007), while in the Sangre de Cristo record, the 9.3 ka event is larger in amplitude in the vegetation (and therefore temperature) records. The 8.2 ka event is more pronounced in the MS profile which suggests a stronger hydrologic response in the basin than the 9.3 ka event. The 9.95 ka anomaly is a short-lived cold event (70–100 yr; Rasmussen et al., 2007) and is a similarly short event in the Sangre de Cristo record. The Preboreal oscillation in core B1-5 occurs at ~11.1 ka which is later than the reported date in Greenland (11.3–11.5 ka; Rasmussen et al., 2007) but lies within the error of the age model for the core.

Alternations in peaks of Poaceae and Cyperaceae pollen during the last 3000 yr of the Holocene also suggest substantial climate variability at Stewart Bog. We interpret increases in Poaceae as reflecting a drying of the bog surface, while increases in Cyperaceae reflect higher water tables. Major peaks in Poaceae are centred on ca 2.3, 1.7, 1.0 and 0.35 ka. Several of these peaks are coincident with droughts inferred from speleothem growth, which is directly affected by groundwater availability. For instance, speleothem growth at Hidden Cave in southern New Mexico was arrested between ca 1.7–1.3 ka, and after ca 0.9–0.8 ka (Polyak and Asmerom, 2001; Polyak et al., 2001), and centred around 0.8–1.2 and 2.1–2.3 ka at Carlsbad Cavern (Rasmussen et al., 2006).

Even though generally good correspondence appears to exist between the different proxies from Stewart Bog and those from hemispheric and cosmic sources, some discrepancies are apparent. For example, a poor correlation exists between the subalpine tree pollen and MS records between ca 8.2 and 7.4 ka. Pollen data suggest cooler temperatures during the entire period, which could correspond to either cold events 5 or 5a (the so-called 8.2 ka event) of Bond et al. (2001). However, MS data suggest a more limited temporal extent for this event with low values only between 8.1 and 7.8 ka (Fig. 5H). We believe that this strengthens an interpretation as the 8.2 ka event being the most-likely possible climate forcing. Another example is the decrease in MS at ~11 ka, which could be correlated with cold event 8, but only appears to correspond to a decrease in the P/A ratio (Fig. 5G) and not to an important decrease in subalpine conifer trees in the pollen spectra (Fig. 5F). In general, we can ascribe these discrepancies to several factors, including (a) minor age offsets

between the records resulting from the uncertainty of radiocarbon dating (Table 1); (b) a delay in vegetation response after a climate change (Shuman et al., 2005); or (c) regional vegetation/climatic variability.

In order to test for the presence of cyclical variations in our pollen record, we used a cyclostratigraphic analysis on the raw B1-5 relative subalpine conifer tree pollen abundance time series using the program REDFIT (Schultz and Mudelsee, 2002). Our analysis documented millennial- and centennial-timescale periodicities of 197, 212, 222, 292, 735 and 5750 yr above the 90% confidence level (CL; Fig. 7A). Several of these periodicities coincide with known solar cycles and are in agreement with previous studies that show centennial-scale variability in Holocene climatic records from widely dispersed geographic regions. For example, the 197, 212 and 222-yr (all above 95% CL) periods are very similar to the 208-yr Suess cycle in ^{14}C and ^{10}Be production (Damon and Sonnett, 1991). This cycle has been demonstrated from many proxies in the North Atlantic marine record (Bond et al., 2001) and elsewhere worldwide (e.g., Peterson et al., 1991; Scuderi, 1993; Hodell et al., 2001; Hu et al., 2003; Poore et al., 2003). Periods around 300 yr have also been documented in subpolar North Atlantic ice rafting debris records (Bond et al., 2001) and in the Gulf of Mexico (Poore et al., 2003). The 735-yr cycle is very similar to the ~800 yr in ^{14}C production (power spectrum shown in Dean et al., 2002) and even though it has not been widely reported in other records, as it is half of the ~1500-yr cycle shown in several previous studies (Bond et al., 2001; Viau et al., 2002; Hu et al., 2003; Gupta et al., 2005; Asmeron et al., 2007), it could be related to the result of amplitude modulation of the ~1500-yr cycle. Although we recognize a 5750 yr periodicity in our analysis, the fact that only a little over two full cycles (~14 ka) are represented in the Stewart Bog record precludes a definitive assessment of this cycle. However, similar periodicities are common in many records of much longer duration (Chapman and Shackleton, 1999; Luo et al., 2005; Jiménez-Moreno et al., 2007).

Cross-spectral analysis (using SPECTRUM; Schulz and Stattegger, 1997) of the P/A ratio and MS from core B1-5 confirms that the two records have matching periodicities at 200, 358, 531, 793, 1100 and 1592 yr above the false alarm level (Fig. 7B). The coherence between the two records confirms the close relationship between vegetation and sedimentation changes in Stewart Bog over the past 14 ka, also observed by the high positive correlation coefficients calculated for most of the record (Fig. 6). The 200, 531, 793 and 1592 yr peaks are very similar to the spectral peaks (208, 504, 800 and 1500 yr) of the solar variability (Damon and Sonnett, 1991; Bond et al., 2001), which again could point to a relationship between climate in New Mexico and solar variability during the Holocene. Cross-spectral analysis of the residual $\Delta^{14}C$ data (Reimer et al., 2004) and detrended subalpine conifer tree pollen abundance from core B1-5 confirms that the two records have matching periodicities at 200 and 645 yr above the CL (Fig. 7C). The 200-yr coherent peak is very similar to the 208-yr Suess cycle in ^{14}C production (power spectrum shown in Dean et al., 2002) and has been attributed to solar variability (Damon and Sonnett, 1991), also suggesting some relationship between climate in New Mexico and solar variability during the Holocene.

These climate correlations between the American southwest and the North Atlantic basin could suggest a hemispheric footprint for Holocene climate change. Elucidating the specific nature of teleconnections between the southwest and the North Atlantic is not straightforward as the southwest (New Mexico) is primarily impacted by winter frontal weather systems from the Pacific and summer monsoonal rains (probably affected by both the Atlantic and Pacific). If, as we suggest here, the

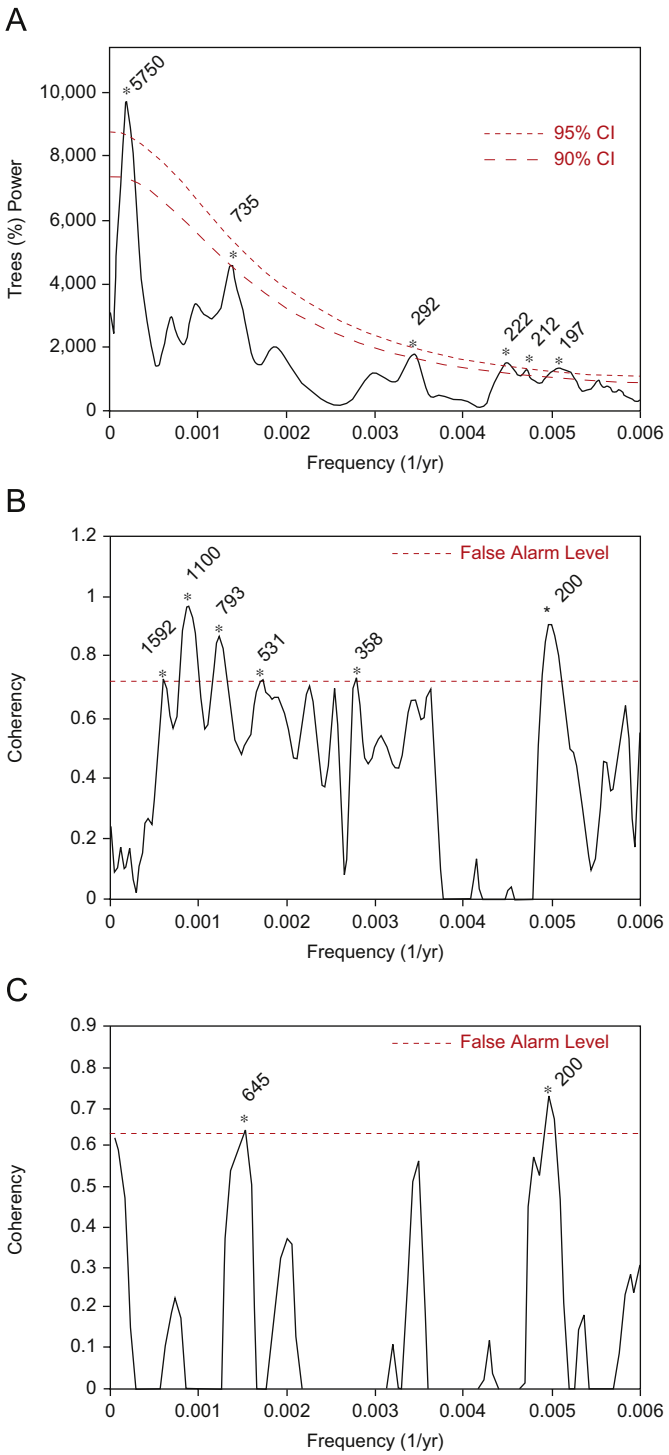

Fig. 7. (A) Spectral analysis of the B1-5 raw pollen time series on subalpine tree taxa (*Abies*, *Picea* and *Pinus*). The confidence intervals (90% and 95%) are shown by different lines. Significant periodicities (above the 90% confidence level) are marked. The spectral analysis was done using REDFIT (Schultz and Mudelsee, 2002). A number of overlapping (50%) segments (n_{seg}) of 3 and Hanning type spectral window were used. (B) Coherency from cross-spectral analysis of the P/A ratio and the MS from core B1-5. Significant peaks above the false alarm level (dashed horizontal line; $\alpha = 0.1$) are shown. (C) Coherency from cross-spectral analysis of the detrended relative abundance of tree taxa (*Abies*, *Picea* and *Pinus*) from core B1-5 and residual $\Delta^{14}C$ data calculated from IntCal04 $\Delta^{14}C$ (‰) with a 2000-yr moving average subtracted signal (INTCAL04; Reimer et al., 2004). Dashed horizontal line indicates false alarm level ($\alpha = 0.1$). Significant peaks above the false alarm level are shown. The cross-spectral analyses were done using SPECTRUM (Schulz and Stattegger, 1997) using the same parameters as for the calculation of the univariate spectral analysis. Tree pollen data was detrended linearly using Analyseries software (Paillard et al., 1996).

centennial-scale changes are primarily the result of solar forcing of temperature, then the hemispheric connection makes sense. Recent work has suggested that small variations in solar output on millennial, centennial and decadal timescales have influenced climate during the Holocene (Stuiver et al., 1998; Bond et al., 2001; Hodell et al., 2001; Hu et al., 2003; Gupta et al., 2005; Asmeron et al., 2007). However, the amplitude of temperature changes directly related to solar change is unknown (Rind, 2002) and may be smaller than that suggested by the vegetation and treeline changes.

Recent work has also suggested a role for changes in North Atlantic thermohaline circulation and attendant changes in Atlantic basin sea-surface temperature gradients on Pacific ENSO variability (Dong et al., 2006; Timmermann et al., 2007; Dong and Sutton, 2007). It has also been suggested that the Atlantic Multidecadal Oscillation (AMO) can modulate large-scale patterns of precipitation variability in the western US, including summer precipitation and winter precipitation variability associated with El Nino—southern Oscillation (Enfield et al., 2001; McCabe et al., 2004). These kinds of teleconnections between the Atlantic and Pacific might help to explain the correlation between the Sangre de Cristo Mountains and the North Atlantic for that part of the record due to changes in precipitation and basin hydrology.

4. Conclusions

The high-resolution pollen record presented here documents variations in subalpine tree pollen and P/A ratios, suggesting changes in alpine treeline caused by climate change. These fluctuations generally co-vary with changes in MS, denoting changes in the clastic deposition in the basin that are related to similar climatic forcing factors.

Pollen and MS records show lowest alpine treeline and MS during the end of the Pinedale glaciation and the Younger Dryas chrons. A long-term warming trend is observed during the early Holocene until ~5.6 ka, when the warmest climate and highest alpine treeline were recorded. Following this is a progressive and slight climate cooling occurring until today. These climate changes are mainly associated with orbital-scale variations in Earth's insolation, the decreasing size of the Laurentide Ice Sheet and changes in atmosphere CO_2 concentration.

The Holocene climatic fluctuations observed in our pollen and MS records may reflect a manifestation of climatic cycles related to variations in solar activity on centennial-timescales as shown by the correlation with residual ^{14}C record and a prominent 208 yr cycle in vegetation and MS throughout the Holocene. The main vegetation changes appear to be synchronous with transitions in marine records from the North Atlantic and other regions of the world. The high resolution of this vegetation record also allows the recognition of several early Holocene cold events that probably correspond to the Preboreal Oscillation, the 9.95 ka climate anomaly, and the 9.3 and 8.2 ka climate events, in addition to the middle and late Holocene climate changes recognized by Armour et al. (2002). The vegetation record in this area supports the conclusion that high-frequency climatic variability during the Holocene is probably a hemisphere-wide phenomena.

Acknowledgements

GJM's research was supported by a postdoctorate grant from the Universidad de Granada (Spain). We thank Jake Armour for the MS data, Grant Meyer and Jed Frechette for discussions and Lee Nordt, Julio Betancourt and two anonymous reviewers for helpful comments on the manuscript. Partial funding for radiocarbon analysis came from IGPP LANL and NSF (to P.J.F.) and funding for pollen processing came from the USGS Western Mountain Intitiative (to R.S.A.)

References

Allen, R.B., Peet, R.K., 1990. Gradient analysis of forests in the Sangre de Cristo Range, Colorado. Canadian Journal of Botany 68, 193–201.
Alley, R.B., Mayewski, P.A., Sowers, T., Stuiver, M., Taylor, K.C., Clark, P.U., 1997. Holocene climatic instability: a prominent, widespread event 8200 yr ago. Geology 25, 483–486.
Anderson, R.S., Smith, S.J., 1994. Paleoclimatic interpretations of meadow sediment and pollen stratigraphies from California. Geology 22, 723–726.
Anderson, R.S., Hasbargen, J., Koehler, P.A., Feiler, E.J., 1999. Post-glacial and Holocene subalpine forests on the Markagunt Plateau, southwestern Colorado Plateau, Utah. Arctic, Antarctic and Alpine Research 31, 367–378.
Anderson, R.S., Allen, C.D., Toney, J.L., Jass, R.B., Bair, A.N., 2008a. Holocene vegetation and fire regimes in subalpine and mixed conifer forests, southern Rocky Mountains, USA. International Journal of Wildland Fire 17, 96–114.
Anderson, R.S., Jass, R.B., Toney, J.L., Allen, C.D., Ciseros-Dozal, L.M., Hess, M., Heikoop, J., Fessenden, J., 2008b. Development of mixed conifer forest in northern New Mexico, and its relationship to Holocene environmental change. Quaternary Research 69, 263–275.
Armour, J., Fawcett, P.J., Geissman, J.W., 2002. 15 kyr paleoclimatic and glacial record from northern New Mexico. Geology 30, 723–726.
Asmeron, Y., Polyak, V., Burns, S., Rassmussen, J., 2007. Solar forcing of Holocene climate: new insights from a speleothem record, southwestern United States. Geology 35, 1–4.
Bond, G.C., Kromer, B., Beer, J., Muscheler, R., Evans, M., Showers, W., Hoffmann, S., Lotti-Bond, R., Hajdas, I., Bonani, G., 2001. Persistent solar influence on North Atlantic climate during the Holocene. Science 294, 2130–2136.
Cairns, D.M., Malanson, G.P., 1998. Environmental variables influencing the carbon balance at the alpine treeline: a modeling approach. Journal of Vegetation Science 9, 679–692.
Carrara, P.E., Mode, W.N., Rubin, M., 1984. Deglaciation and postglacial timberline in the San Juan Mountains, Colorado. Quaternary Research 21, 42–55.
Carrara, P.E., Trimble, D.A., Rubin, M., 1991. Holocene treeline fluctuations in the northern San Juan Mountains, Colorado, USA, as indicated by radiocarbon-dated conifer wood. Arctic and Alpine Research 23, 233–246.
Castiglia, P.J., Fawcett, P.J., 2006. Large Holocene lakes and climate change in the Chihuahuan desert. Geology 34, 113–116.
Chapman, M.R., Shackleton, N.J., 1999. Global ice-volume fluctuations, North-Atlantic ice-rafting events, and deep-ocean circulation changes between 130 and 70 ka. Geology 27, 795–798.
Damon, P.E., Sonnett, C.P., 1991. Solar and terrestrial components of the atmospheric ^{14}C variation spectrum. In: Sonett, C.P., Giampapa, M.S., Matthews, M.S. (Eds.), The Sun in Time. University of Arizona Press, Tucson, AZ, USA.
Davis, O., Shafer, D.S., 1992. A Holocene climatic record for the Sonoran Desert from pollen analysis of Montezuma Well, Arizona, USA. Palaeogeography, Palaeoclimatology, Palaeoecology 92, 107–119.
Dean, W., Anderson, R., Bradbury, J.P., Anderson, D., 2002. A 1500-year record of climatic and environmental change in Elk Lake, Minnesota I: varve thickness and gray-scale density. Journal of Paleolimnology 27, 287–299.
Dick-Peddie, W.A., 1993. New Mexico Vegetation, Past, Present and Future. University of New Mexico Press, Albuquerque.
Dong, B., Sutton, R., 2007. Enhancement of ENSO variability by a weakened Atlantic Thermohaline circulation in a coupled GCM. Journal of Climate 20, 4920–4939.
Dong, B.-W., Sutton, R.T., Scaife, A.A., 2006. Multidecadal modulation of El Niño—Southern Oscillation (ENSO) variance by Atlantic Ocean sea surface temperatures. Geophysical Research Letters 33, L08705.
Enfield, D.B., Mestas-Nunez, A.M., Timble, P.J., 2001. The Atlantic multidecadal oscillation and its relation to rainfall and river flows in the continental US. Geophysical Research Letters 28, 2077–2080.
Faegri, K., Iversen, J., 1989. Textbook of Pollen Analysis, IV ed. Wiley, New York.
Fall, P.L., 1992. Pollen accumulation in a montane region of Colorado, USA: a comparison of moss polsters, atmospheric traps, and natural basins. Review of Palaeobotany and Palynology 72, 169–197.
Feiler, E.J., Anderson, R.S., Koehler, P.A., 1997. Late Quaternary paleoenvironments of the White River Plateau, Colorado, USA. Arctic and Alpine Research 29, 53–62.
Frechette, J., 2007. Millennial-scale changes in fan deposition and fire severity in ponderosa pine forest, Sacramento Mountains, New Mexico. M.S. Thesis, University of New Mexico, Albuquerque, USA.
Friddell, J.E., Thunell, R.C., Guilderson, T.P., Kashgarian, M., 2003. Increased northeast Pacific climatic variability during the warm middle Holocene. Geophysical Research Letters 30 (11).
Friedman, I., Carrara, P., Gleason, J., 1988. Isotopic evidence of Holocene climatic change in the San Juan Mountains, Colorado. Quaternary Research 30, 350–353.
Gray, S.T., Betancourt, J.L., Jackson, S.T., Eddy, R., 2006. Role of multidecadal climate variability in a range extension of pinyon pine. Ecology 87, 1124–1130.
Grimm, E.C., 1987. CONISS: a FORTRAN 77 program for stratigraphically constrained cluster analysis by the method of incremental sum of squares. Computers and Geosciences 13, 13–35.

Gupta, A.K., Das, M., Anderson, D.M., 2005. Solar influence on the Indian summer monsoon during the Holocene. Geophysical Research Letters 32, L17703.
Hall, S.A., 1990. Pollen deposition and vegetation in the southern Rocky Mountains and southwest Plains, USA. Grana 29, 47–61.
Hodell, D.A., Brenner, M., Curtis, J.H., Guilderson, T., 2001. Solar forcing of drought frequency in the Maya lowlands. Science 292, 1367–1370.
Holmgren, C.A., Norris, J., Betancourt, J.L., 2007. Inferences about winter temperatures and summer rains from the late Quaternary record of C4 perennial grasses and C3 desert shrubs in the northern Chihuahuan Desert. Journal of Quaternary Science 22, 141–161.
Hu, F.S., Kaufman, D., Yoneji, S., Nelson, D., Shemesh, A., Huang, Y., Tian, J., Bond, G., Clegg, B., Brown, T., 2003. Cyclic variation and solar forcing of Holocene climate in the Alaskan subartic. Science 301, 1890–1893.
Jiménez-Moreno, G., Anderson, R.S., Fawcett, P.J., 2007. Millennial-scale vegetation and climate changes of the past 225 kyr from western North America. Quaternary Science Reviews 26, 1713–1724.
Johnson, S.J., Dahl-Jensen, D., Gundestrup, N., Steffensen, J.P., Clausen, H.B., Miller, H., Masson-Delmotte, V., Sveinbjornsdottir, A.E., White, J., 2001. Oxygen isotope and palaeotemperature records from six Greenland ice-core stations: Camp Century, DYE-3, GRIP, GISP2, Renland, and NorthGRIP. Journal of Quaternary Science 16, 299–307.
Kaufman, D.S., Ager, T.A., Anderson, N.J., Anderson, P.M., Andrews, J.T., Bartlein, P.J., Brubaker, L.B., Coats, L.L., Cwynar, L.C., Duvall, M.L., Dyke, A.S., Edwards, M.E., Eisner, W.R., Gajewski, K., Geirsdóttir, A., Hu, F.S., Jennings, A.E., Kaplan, M.R., Kerwin, M.W., Lozhkin, A.V., MacDonald, G.M., Miller, G.H., Mock, C.J., Oswald, W.W., Otto-Bliesner, B.L., Porinchu, D.F., Rühland, K., Smol, J.P., Steig, E.J., Wolf, B.B., 2004. Holocene thermal maximum in the western Arctic (0–180°W). Quaternary Science Reviews 23, 529–560.
Kutzbach, J., Gallimore, R., Harrison, S., Behling, P., Selin, R., Laarif, F., 1998. Climate and biome simulations for the past 21,000 years. Quaternary Science Reviews 17, 473–506.
Laskar, J., 1990. The chaotic motion of the solar system—a numerical estimate of the size of the chaotic zones. Icarus 88, 266–291.
Luo, Y., Sun, X., Jian, Z., 2005. Environmental change during the penultimate glacial cycle: a high-resolution pollen record from ODP Site 1144, South China Sea. Marine Micropaleontology 54, 107–123.
Maher, L., 1972. Nomograms for computing 0.95 confidence limits of pollen data. Review of Palaeobotany and Palynology 13, 85–93.
Markgraf, V., Scott, L., 1981. Lower timberline in central Colorado during the past 15,000 yr. Geology 9, 231–234.
McCabe, G.J., Palecki, M.A., Betancourt, J.L., 2004. Pacific and Atlantic Ocean influences on multidecadal drought frequency in the United States. Proceedings of the National Academy of Sciences 101, 4136–4141.
Menking, K.M., Anderson, R.Y., 2003. Contributions of La Niña and El Niño to middle Holocene drought and late Holocene moisture in the American southwest. Geology 31, 937–940.
Moy, C.M., Seltzer, G.O., Rodbell, D.T., Anderson, D.M., 2002. Variability of El Niño/Southern Oscillation activity at millennial timescales during the Holocene epoch. Nature 420 (6912), 162–165.
Nordt, L., von Fischer, J., Tieszen, L., 2007. Late Quaternary temperature record from buried soils of the North American Great Plains. Geology 35, 159–162.
Paillard, D., Labeyrie, L., Yiou, P., 1996. Macintosh program performs time-series analysis. Eos Transactions AGU 77, 379.
Peet, R.K., 1988. Forests of the Rocky Mountains. In: Barbour, M.G., Billings, W.D. (Eds.), North American Terrestrial Vegetation. Cambridge University Press, New York, pp. 63–101.
Peterson, L.C., Overpeck, J.T., Kipp, N.G., Imbrie, J., 1991. A high-resolution Late Quaternary upwelling record from the anoxic Cariaco Basin, Venezuela. Paleoceanography 6, 99–119.
Pierce, J.L., Meyer, G.A., 2008. Long-term fire history from alluvial fan sediments: the role of drought and climate variability, and implications for management of Rocky Mountain forests. International Journal of Wildland Fire 17, 84–95.
Pierce, J.L., Meyer, G.A., Timothy Jull, A.J., 2004. Fire-induced erosion and millennial-scale climate change in northern Ponderosa pine forest. Nature 432, 87–90.
Polyak, V.J., Asmerom, Y., 2001. Late Holocene climate and cultural changes in the southwestern United States. Science 294 (5540), 148–151.
Polyak, V.J., Cokendolpher, J.C., Norton, R.A., Asmerom, Y., 2001. Wetter and cooler late Holocene climate in the southwestern United States from mites preserved in stalagmites. Geology 29 (7), 643–646.
Poore, R.Z., Dowsett, H.J., Verardo, S., Quinn, T.M., 2003. Millennial- to century-scale variability in Gulf of Mexico Holocene climate records. Paleoceanography 18 (2), 1048.
Rasmussen, J.B.T., Polyak, V.J., Asmerom, Y., 2006. Evidence for Pacific-modulated precipitation variability during the late Holocene from the southwestern USA. Geophysical Research Letters 33, L08701.
Rasmussen, S.O., Vinther, B.M., Clausen, H.B., Anderson, K.K., 2007. Early Holocene climate oscillations recorded in three Greenland ice cores. Quaternary Science Reviews 26, 1907–1914.
Reasoner, M.A., Jodry, M.A., 2000. Rapid response of alpine timberline vegetation to the younger Dryas climate oscillation in the Colorado Rocky Mountains, USA. Geology 28, 51–54.
Reimer, P.J., Baillie, M.G.L., Bard, E., Bayliss, A., Beck, J.W., Bertrand, C., Blackwell, P.G., Buck, C.E., Burr, G., Cutler, K.B., Damon, P.E., Edwards, R.L., Fairbanks, R.G., Friedrich, M., Guilderson, T.P., Hughen, K.A., Kromer, B., McCormac, F.G., Manning, S.W., Bronk Ramsey, C., Reimer, R.W., Remmele, S., Southon, J.R., Stuiver, M., Talamo, S., Taylor, F.W., van der Plicht, J., Weyhenmeyer, C.E., 2004. Radiocarbon 46, 1029–1058.
Rein, B., Lückge, A., Reinhardt, L., Sirocko, F., Wolf, A., Dullo, W.-C., 2005. El Niño variability off Peru during the last 22,000 years. Paleoceanography 20, PA4003.
Rind, D., 2002. The Sun's role in climate variations. Science 296, 673–677.
Shafer, D.S., 1989. The timing of Late Quaternary monsoon precipitation maxima in the southwest United States. Ph.D. Dissertation, University of Arizona.
Schulz, M., Stattegger, K., 1997. SPECTRUM: spectral analysis of unevenly spaced paleoclimatic time series. Computers and Geosciences 23, 929–945.
Schultz, M., Mudelsee, M., 2002. REDFIT: estimating red-noise spectra directly from unevenly spaced paleoclimatic time series. Computers and Geosciences 28, 421–426.
Scuderi, L.A., 1993. A 2000-year treering record of annual temperatures in the Sierra Nevada Moutains. Science 259, 1433–1436.
Shuman, B., Bartlein, P.J., Webb III, T., 2005. The magnitudes of millennial- and orbital-scale climatic change in eastern North America during the Late Quaternary. Quaternary Science Reviews 24, 2194–2206.
Stuiver, M., Reimer, P.J., 1993. Extended ^{14}C data base and revised CALIB 3.0 ^{14}C Age calibration program. Radiocarbon 35 (1), 215–230.
Stuiver, M., Reimer, P.J., Bard, E., Beck, J.W., Burr, G.S., Hughen, K.A., Komar, B., McCormac, F.G., Plicht, J.v.d., Spurk, M., 1998. INTCAL98 Radiocarbon age calibration 24,000–0 cal BP. Radiocarbon 40, 1041–1083.
Timmermann, A., Okumura, Y., An, S.-I., Clement, A., Dong, B., Guilyardi, E., Hu, A., Jungclaus, J., Krebs, U., Renold, M., Stocker, T.F., Stouffer, R.J., Sutton, R., Xie, S.-P., Yin, J., 2007. The influence of shutdown of the Atlantic meridional overturning circulation on ENSO. Journal of Climate 20, 4899–4919.
Toney, J.L., Anderson, R.S., 2006. A postglacial palaeoecological record from the San Juan Mountains of Colorado USA: fire, climate and vegetation history. The Holocene 16, 505–517.
Viau, A.E., Gajewski, K., Fines, P., Atkinson, D.E., Sawada, M.C., 2002. Widespread evidence of 1500 yr climate variability in North America during the past 14,000 yr. Geology 30, 455–458.
Weber, W.A., Wittman, R.C., 1996. Colorado Flora: Eastern Slope, revised Edition. University of Colorado Press, Boulder, CO.
Weng, C., Jackson, S.T., 1999. Late-glacial and Holocene vegetation history and paleoclimate of the Kaibab Plateau, Arizona. Palaeogeography, Palaeoclimatology, Palaeoecology 153, 179–201.
Wesling, J.R., 1988. Glacial chronology and soil development in Winsor Creek drainage basin, southernmost Sangre de Cristo Mountains. M.S. Thesis, University of New Mexico, Albuquerque, NM, USA.
Willard, D.A., Bernhardt, C.E., Korejwo, D.A., Meyers, S.R., 2005. Impact of millennial-scale Holocene climate variability on eastern North American terrestrial ecosystems: pollen-based climatic reconstruction. Global and Planetary Change 47, 17–35.